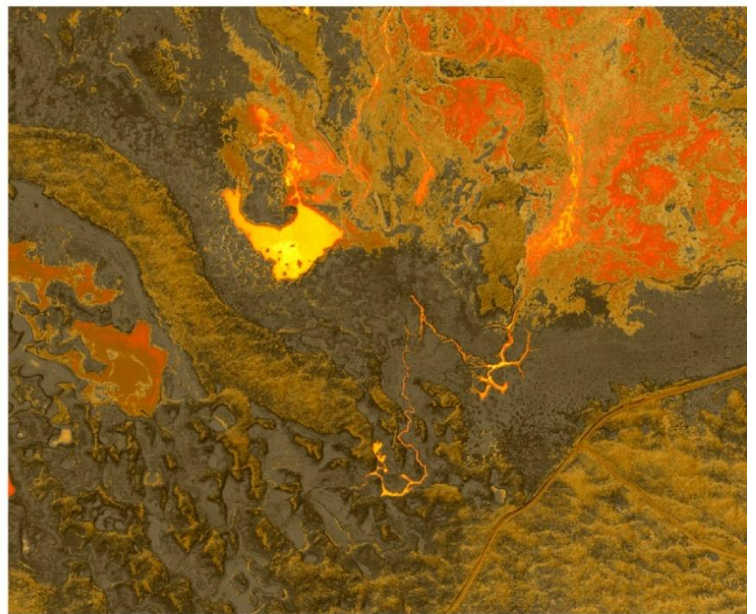
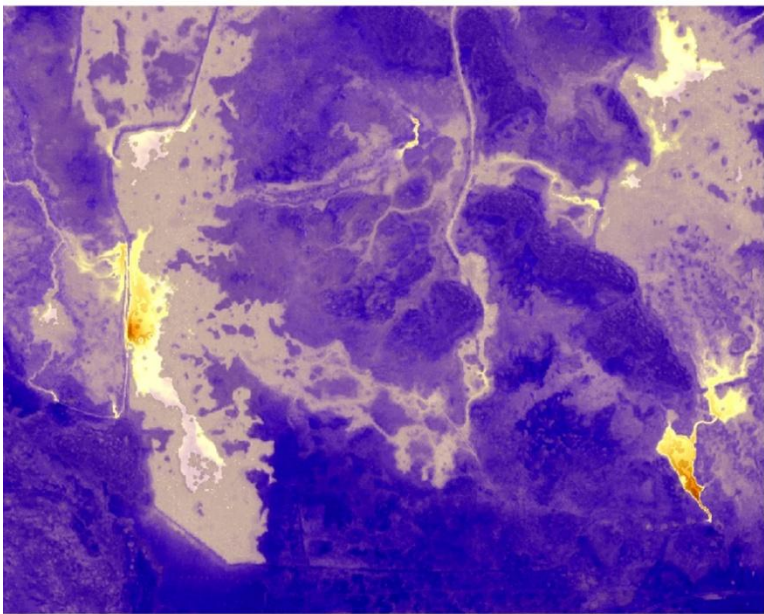
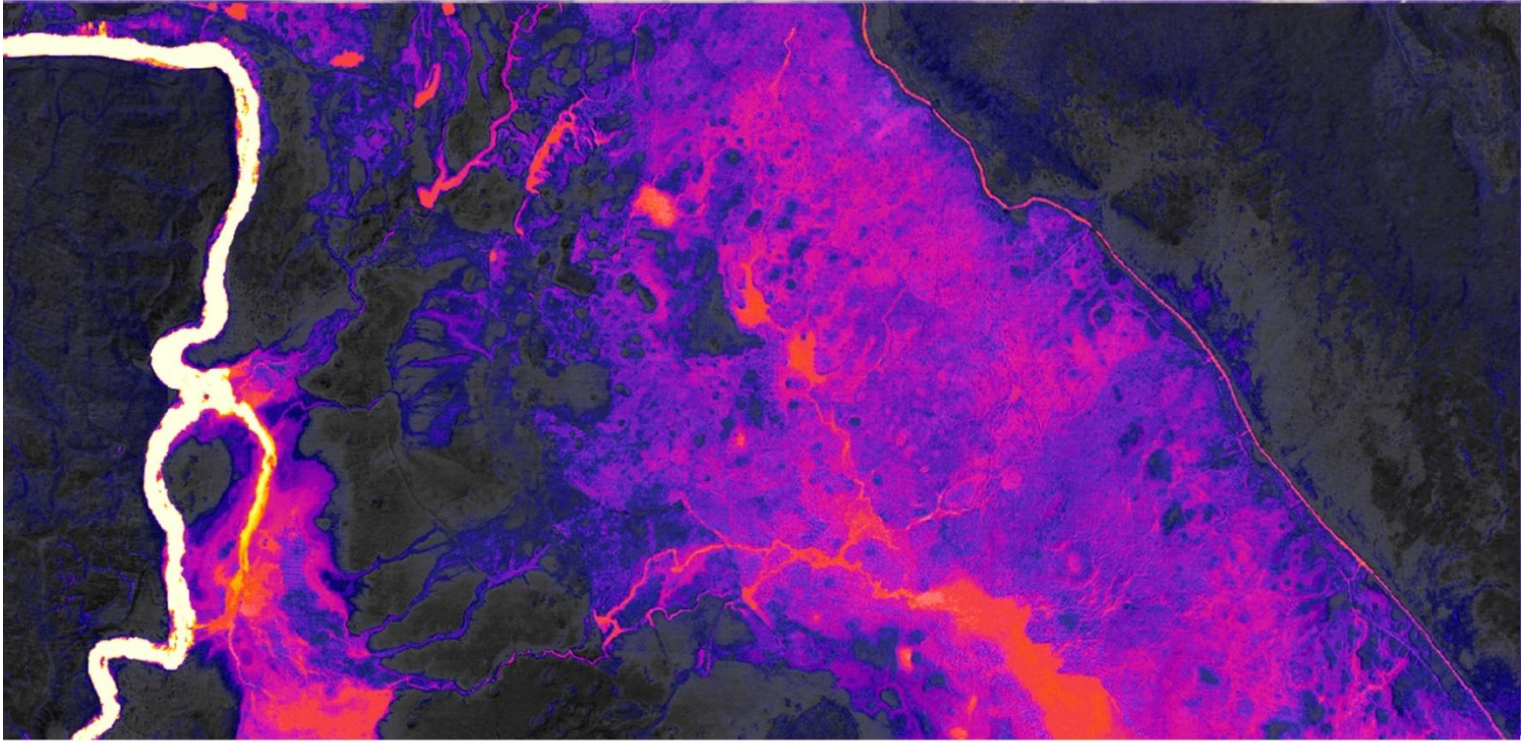


AIRBORNE REMOTE SENSING THERMAL INFRARED & LiDAR

SUMMER LAKE • OREGON

DELIVERY 1



OREGON DEPARTMENT OF GEOLOGY AND MINERAL INDUSTRIES

CLARK NIEWENDORP - 800 NE Oregon St., #28, Suite 965 - Portland, OR 97232



WATERSHED SCIENCES • 517 SW 2nd Street, Suite 400 - Corvallis, OR 97333

DEPARTMENT OF GEOLOGY & MINERAL INDUSTRIES

AIRBORNE REMOTE SENSING: THERMAL INFRARED & LiDAR

DELIVERY 1: SUMMER LAKE, OREGON

TABLE OF CONTENTS

1. Overview	1
2. Thermal Infrared (TIR) Imagery	2
2.1 TIR Acquisition	2
2.1.1 Airborne Instrumentation	2
2.1.2 Ground Control	3
2.1.2.1 Static Survey Data	3
2.1.2.2 Air Targets	4
2.1.3 Acquisition Summary	5
2.1.4 Temperature Calibration	6
2.2 Thermal Image Characteristics	7
2.2.1 Surface Temperatures	7
2.2.2 Expected Accuracy	7
2.2.3 Image Uniformity	7
2.2.4 Temperatures and Color Maps	7
2.3 Data Processing	8
2.3.1 Sensor Calibration	8
2.3.2 Ortho-Rectification of Imagery	9
2.3.3 Kinematic GPS Data	9
2.3.4 Image Rectification Workflow and Applications	9
2.3.5 Spatial Accuracy Assessment	10
2.4 Study Area Results	10
2.4.1 Spatial Accuracy for Thermal Imagery	12
2.4.2 Thermal Accuracy Assessment	12
3. Light Detection and Ranging (LiDAR)	14
3.1 Ground Survey - Instrumentation and Methods	14
3.1.1 Methodology	15
3.2 Data Processing	16
3.2.1 Applications and Work Flow Overview	16
3.2.2 Aircraft Kinematic GPS and IMU Data	17
3.2.3 Laser Point Processing	17
3.3 LiDAR Accuracy Assessment	19
3.3.1 Absolute Accuracy	19
3.3.2 LiDAR Data Summary	19
3.3.3 LiDAR Relative Accuracy Calibration Results	20
3.3.4 LiDAR Absolute Accuracy	20
4. Projection/Datum and Units	21
5. Deliverables	21
5.1 TIR Deliverables	21

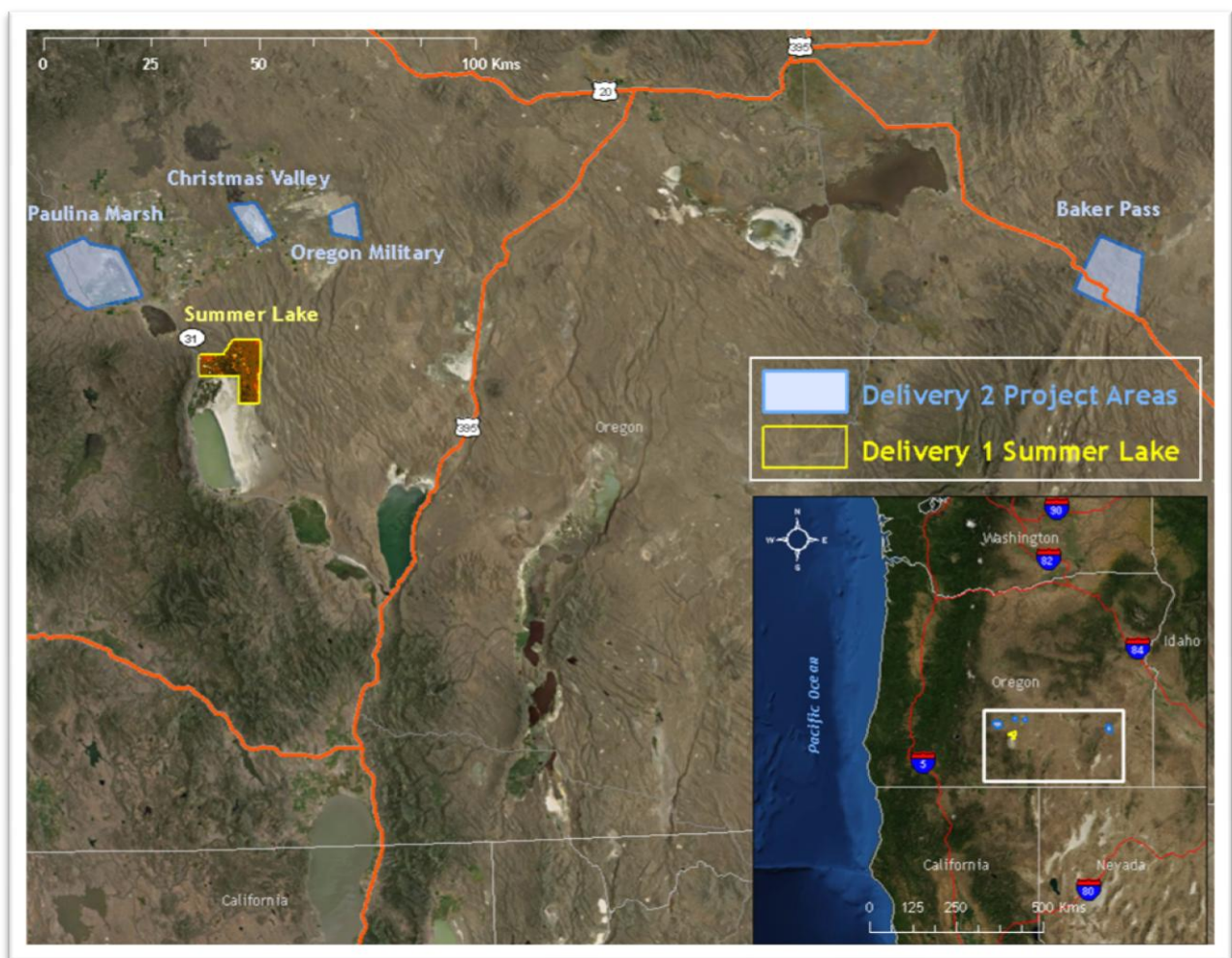
5.2 LiDAR Deliverables.....	21
6. Certifications	22
7. Selected Images	23
8. Glossary.....	28
9. Citations	28

1. Overview

Watershed Sciences, Inc. (WS) collected airborne Thermal Infrared (TIR) imagery and Light Detection and Ranging (LiDAR) data for the Department of Geology and Mineral Industries (DOGAMI) Summer Lake study area on March 4th, 2012. The Summer Lake study area is the first delivery of a larger state wide project that will include 4 more study areas in Delivery 2. The requested area of 29,537 acres was expanded to include a 100m buffer to ensure complete coverage around survey area boundaries. This expansion results in a total of 30,916 acres of delivered TIR and LiDAR data (Figure 1). The TIR imagery provides an accurate data set for detecting and identifying surface expression of geo-thermal activity. LiDAR data was co-acquired with the TIR imagery and provides highly detailed topographic data for recognizing landforms associated with detected thermal features.

Airborne TIR remote sensing has proven to be an effective method for mapping spatial temperature patterns on terrestrial surfaces. The TIR imagery illustrates the location and thermal influence of point sources, terrestrial springs, and evidence of geothermal activity.

Figure 1. The Summer Lake study area consisted of 30,916 delivered acres. The image shows the TIR image and a project specific Kelvin*10 color ramp



Thermal Infrared & LiDAR Remote Sensing: (DOGAMI) Summer Lake, OR

Prepared by Watershed Sciences, Inc.

2. Thermal Infrared (TIR) Imagery

2.1 TIR Acquisition

2.1.1 Airborne Instrumentation

TIR images were collected with a FLIR Systems SC6000 sensor (8-9.2 μ m) mounted in the Cessna Caravan. The SC6000 has a 640x512 QWIP detector array capable of collecting 14-bit digital frames directly from the sensor to an on-board computer. The SC6000 is a calibrated radiometer with a NETD of 0.05°C, internal non-uniformity correction and drift compensation. Images are initially collected in a binary data format representing the measured, emitted radiance in the scene. The TIR sensor has a 50mm lens resulting in a total horizontal field-of-view of 18°. General specifications of the thermal infrared sensor are listed in Table 1.

Thermal infrared images were recorded directly from the sensor to an on-board computer as raw counts, which were then converted to radiant temperatures ($^{\circ}$ K * 10) based on the calibration coefficients of the sensor and the recorded environmental conditions. The individual images were referenced using an IRIG-B time-code generated from an onboard GPS. The aircraft position and attitude (pitch, roll, and yaw) were precisely recorded using an on board GPS/IMU. The image frames were linked to the GPS/IMU data during the post processing.

Table 1. Summary of TIR sensor specifications

Sensor:	FLIR System SC6000 (LWIR)
Wavelength:	8-9.2 μ m
Noise Equivalent Temperature Differences (NETD):	0.035°C
Pixel Array:	640 (H) x 512 (V)
Encoding Level:	14 bit
Horizontal Field-of-View:	18.0°

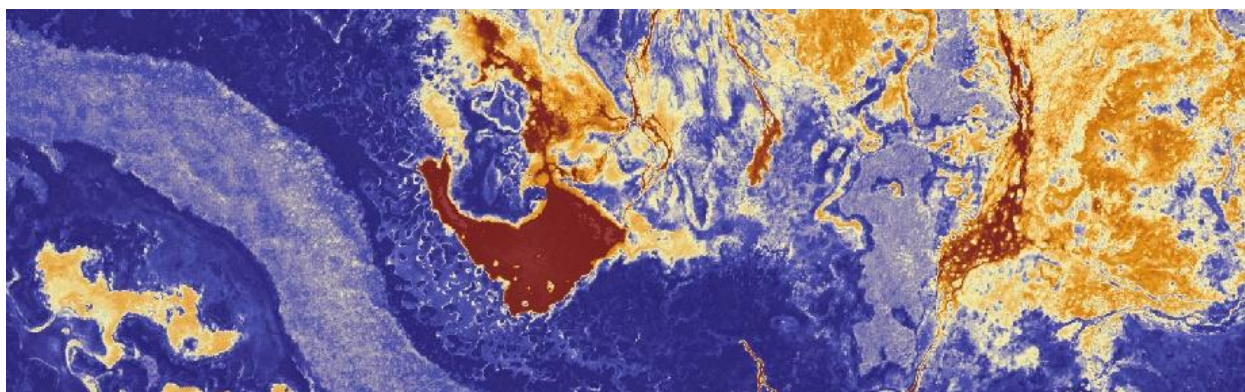




Figure 2 - WSI's FLIR SC6000 integrated with a Leica ALS50-Phase II LiDAR System installed in one of WSI's Cessana Caravans. The SC6000 utilizes the same GPS/IMU system as the LiDAR system for direct computation of image external orientation

2.1.2 Ground Control

2.1.2.1 Static Survey Data

Ground survey data were collected to enable the geo-spatial correction of the aircraft positional coordinate data collected throughout the flight. During the flight, 1 Hz static ground surveys were conducted over monuments using a Trimble GNSS model R7 Zephyr Geodetic Model 2 antenna with ground plane and a Trimble R8 GNSS Model 2 receiver were deployed for all static control (Table 2). All GPS measurements were made with dual frequency L1-L2 receivers with carrier-phase correction.



Watershed Sciences established 2 new monuments for the Summer Lake study area. The monumentation was done with 5/8" x 30" rebar topped with a metal cap stamped with "Watershed Sciences, Inc.," the monument ID, and the year of establishment.

Table 2. Control Monuments for the Summer Lake study area

Base Station ID	Datum: NAD83 (CORS96)		GRS80
	Latitude	Longitude	Ellipsoid Z (meters)
DOGAMI 7	43° 00' 19.91633"	120° 43' 53.26249"	1272.667
DOGAMI 8	42° 57' 54.05452"	120° 38' 56.27157"	1276.375

Thermal Infrared & LiDAR Remote Sensing: (DOGAMI) Summer Lake, OR

Prepared by Watershed Sciences, Inc.

2.1.2.2 Air Targets

Air targets were distributed in the study area in order to quantify the spatial accuracy of geo-rectified TIR imagery. Air targets consisted of space blankets and small, catalytic portable heaters (Figure 4). The target locations were surveyed using real time kinematic (RTK) techniques. The distribution of the air targets are illustrated in Figure 3.

Figure 3. Air target locations deployed for the Summer Lake study area

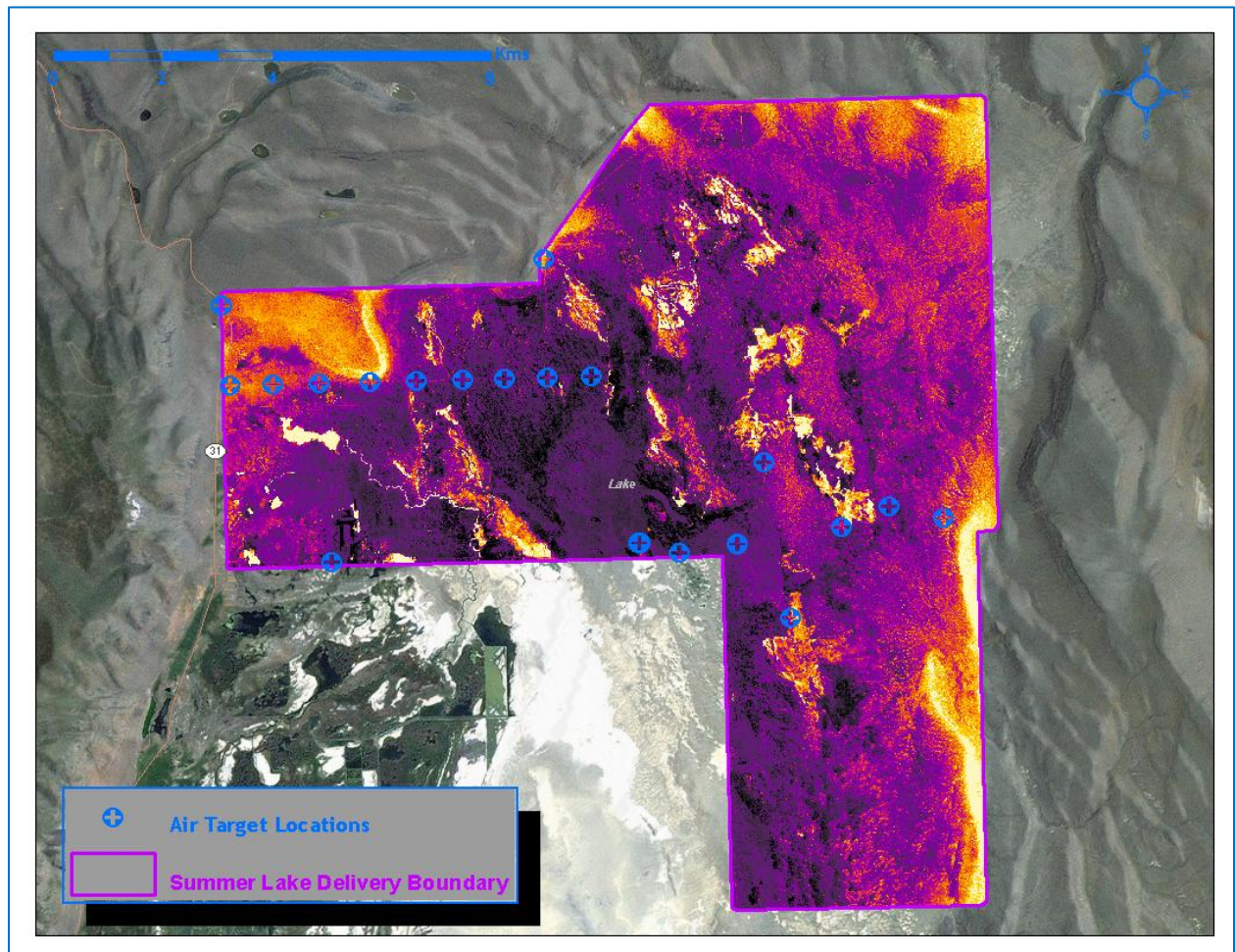




Figure 4. GPS base station set up with “space” blanket target set up near the control monument. The space blanket has a very low emissivity compared to the surrounding terrain and is detectable in the TIR imagery. The blankets were paired with small, catalytic heaters to quantify the accuracy of the TIR mosaic

2.1.3 Acquisition Summary

The aircraft was flown in parallel flight lines in order to capture the entire requested area. The flight lines were designed for an image side-lap of 40% while the TIR sensor was set to acquire images at a rate of 1 image every second resulting in an image overlap of approximately 60%. The TIR data acquisition was conducted at a flight altitude of 1100 meters above ground level (AGL) resulting in a native pixel resolution of 0.5m. A summary of acquisition parameters and flight times can be seen in Table 3.

Flight planning was developed to capture the greatest possible temperature difference between geothermal sources and ambient temperatures of the surrounding landscape. Acquisition began shortly after midnight and was completed just before dawn (*Environmental information reported below (Table 3) from the “Weather Underground” website as recorded in Lakeview, OR (<http://www.wunderground.com/>)*).

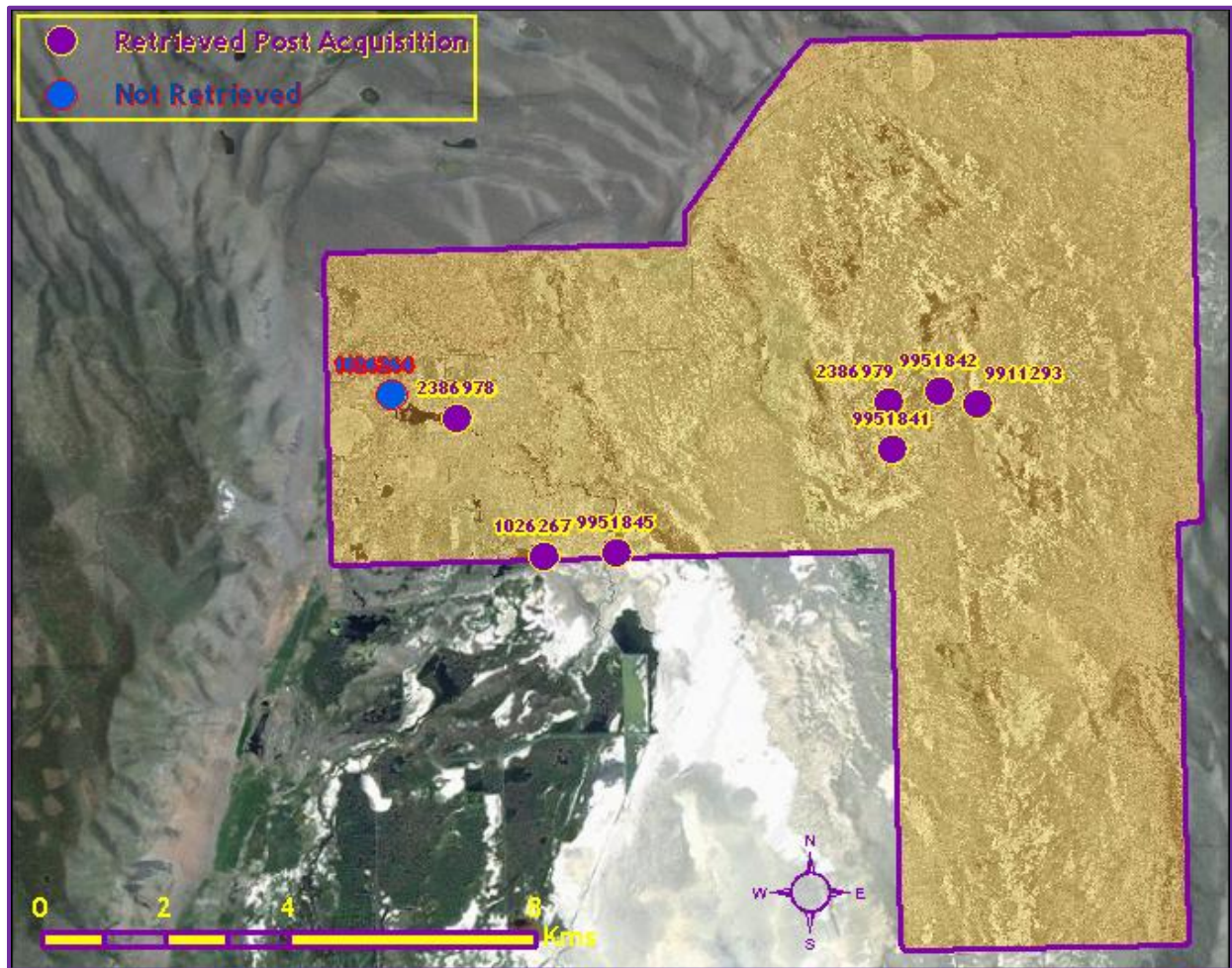
Table 3. Flight times and weather conditions of the March 4th, 2012 co-acquisition of the Summer Lake study area

Acquisition Time	00:34-06:07 hrs
Sunrise	06:30 hrs
Ambient Temperatures	00:00hrs = 23°F, 06:00hrs = 17°F
Frames Captured	10,794 image frames
Flight Altitude	1,100 meters
Native Pixel Size	0.5 meters

2.1.4 Temperature Calibration

Watershed Sciences, Inc. (WSI) deployed 8 data loggers (Onset Hobo-Pros) during the time frame of the flight for calibrating and verifying the thermal accuracy of the TIR imagery. The WSI Hobo Pro data loggers were set to record temperatures at 10 minute intervals and suspended in the water throughout the study area. The data loggers were deployed on March 3rd, 2012, and retrieved after the entire study area had been acquired on March 4th. Of the 8 data loggers deployed, 7 were successfully recovered. All data logger locations and their respective serial numbers can be found in Figure 5.

Figure 5. Hobo Data Logger locations and serial numbers in the Summer Lake study area



2.2 Thermal Image Characteristics

2.2.1 Surface Temperatures

The TIR imagery was flown just prior to dawn so that terrestrial temperatures would be cool relative to any hot springs. The objective was to achieve the maximum thermal contrast between terrestrial features and surface springs or geothermal anomalies. In the pre-dawn hours, hot springs and other surface expression of geothermal activity should be the warmest features within the thermal infrared scene. Since water is essentially opaque to TIR wavelengths, the sensor is only measuring water surface temperatures. The imagery will clearly show thermal plumes for surface springs or near surface activity, however detection of sub-surface discharge will depend on depth and vertical mixing rates at that location.

2.2.2 Expected Accuracy

Thermal infrared radiation received at the sensor is a combination of energy emitted from the water surface, reflected from the water's surface, and absorbed and re-radiated by the intervening atmosphere. Water is a good emitter of TIR radiation and has relatively low reflectivity (~ 4 to 6%). Surface conditions and atmospheric conditions (path length transmission) can result in some variability in the resulting radiant temperature measurements. In general, radiant temperatures may show frame-to-frame thermal variability of up to 0.5°C

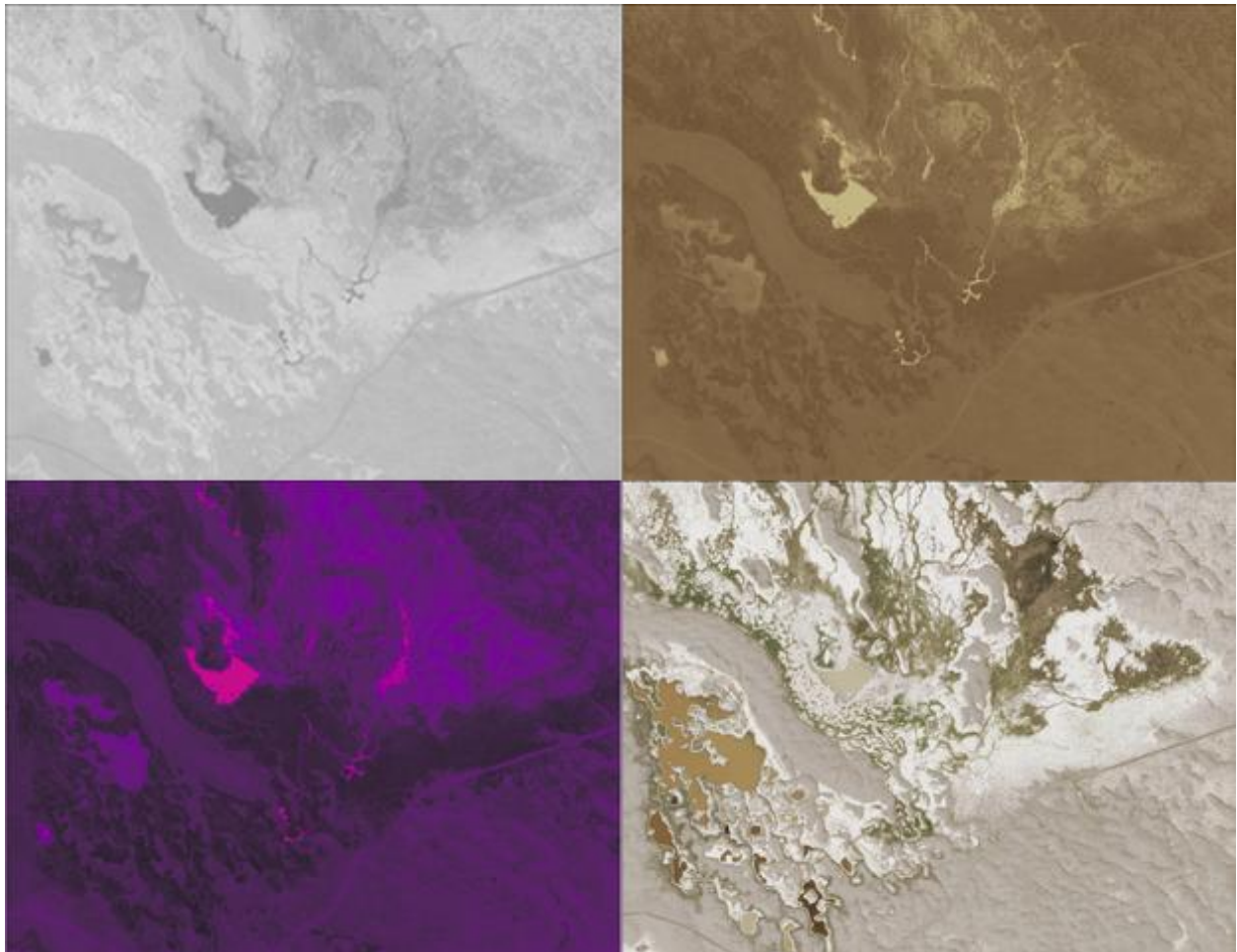
2.2.3 Image Uniformity

The TIR sensor deployed for this study used a focal plane array of detectors to sample incoming radiation. A challenge when using this technology is to achieve uniformity across the detector array. The sensor has a correction scheme which reduces non-uniformity across the image frame. However, differences in temperature can be observed near the edge of the image frame. During processing, we trim the image frames by at least 10% in order to minimize the impact of non-uniformity near the frame edge. Interpretation of the TIR images should consider the inherent thermal variability within the image and use caution when interpreting thermal differences less than ~0.5°C unless they are associated with a distinct thermal discharge.

2.2.4 Temperatures and Color Maps

The TIR images collected during this survey consist of a single band. As a result, visual representation of the imagery (*in a report or GIS environment*) requires the application of a color map or legend for the pixel values. The selection of a color map should highlight features most relevant to the analysis (i.e. *identify geo thermal activity within the project area*). For example, a continuous, gradient style color map that incorporates all temperatures in the image frame will provide a smoother transition in colors throughout the entire image, but may not highlight changes of temperature at a localized scale and fail to identify source sites. Conversely, a color map that focuses too narrowly cannot be applied to the entire project area and will washout relevant features (Figure 6).

Figure 6. Color ramp comparison of a ground spring section of the Summer Lake study area (bottom right corner is 2011 NAIP of Lake County, the remaining images are all thermal mosaics with different color ramps to demonstrate contrast variability)



2.3 Data Processing

2.3.1 Sensor Calibration

The response characteristics of the TIR sensor are measured in a laboratory environment. The response curves relate the raw digital numbers recorded by the sensor to emitted radiance from a black body. The raw TIR images collected during the survey initially contain digital numbers which are then converted to radiance temperatures based on the factory calibration.

The calculated radiant temperatures are adjusted based on the kinetic temperatures recorded at each ground truth location. This adjustment is performed to correct for path length attenuation and the emissivity of natural water. The data are assessed at the time the image is acquired, with radiant values representing the median of ten points sampled from the image at the data logger location.

2.3.2 Ortho-Rectification of Imagery

Light Detection and Ranging (LiDAR) data was collected simultaneously with the TIR flight (*LiDAR methods and results are included in Section 3 of this report*). The following data layers were derived from the LiDAR data and used in TIR image processing:

- 1 meter pixel resolution bare-earth digital surface model (DEM): Used for ortho-rectification of the TIR imagery.
- 0.5 meter pixel resolution LiDAR intensity image: Used for the QA/QC of the final TIR mosaic and assist in the measurement of ground targets during accuracy assessment.

2.3.3 Kinematic GPS Data

While surveying, the aircraft collects kinematic GPS data and the onboard inertial measurement unit (IMU) collects aircraft attitude data. The positional datasets are referenced to static ground GPS that are set up prior to the TIR survey flight. IPAS-TC is used to process the kinematic corrections for the aircraft. The static and kinematic GPS data are then post-processed after the survey to obtain accurate GPS solution and aircraft positions during times of the survey. IPAS-TC is used to develop a trajectory file that includes corrected aircraft position and attitude information. The trajectory data for the entire flight survey session is incorporated into a final smoothed best estimate of trajectory (SBET) file that contains accurate and continuous aircraft positions and attitudes. An exterior orientation file is derived from the SBET file by calculating GPS positions and orientation angles of the sensor at each image capture time and applying lever arm and misalignment angle offsets.

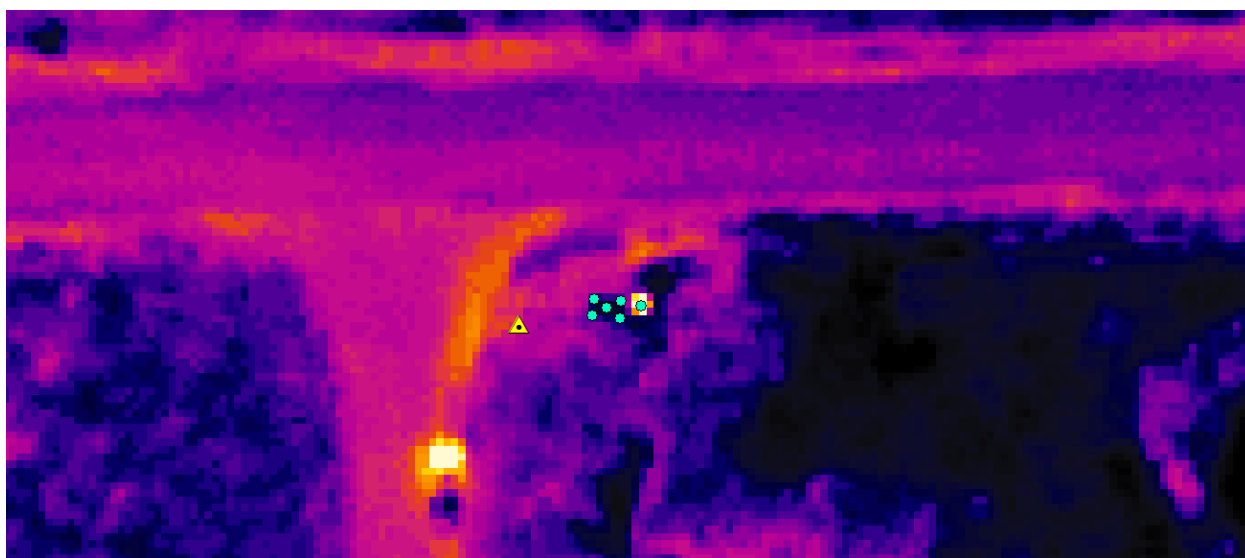
2.3.4 Image Rectification Workflow and Applications

1. Monument static GPS data are processed with aircraft GPS data to resolve kinematic corrections.
Software: IPAS-TC
2. Aircraft attitude data are incorporated with the post processed aircraft kinematic GPS data.
Software: IPAS-TC
3. For each camera exposure event, an exterior orientation is calculated for the perspective center (image center point position X,Y,Z) and orientation angles of the image (omega, phi, kappa), which describe the relationship between the camera mapping frame and the ground.
Software: IPAS-CO
4. Integrated photogrammetric processing of the TIR images. Interior orientation of the FLIR sensor were derived and input into LPS. LPS applies the exterior orientation to images. Ortho-rectification resampling was performed through LPS using the LiDAR derived bare-earth model for elevation values. Images were resampled (nearest neighbor technique) at a ground sample distance of 0.5 meters.
Software: LPS
5. Automatic seam generation and mosaic creation from thermal-images. No adjustments were made to color or contrast so temperature information was preserved.
Software: OrthoVista

2.3.5 Spatial Accuracy Assessment

For the Summer Lake study area 28 air targets were deployed and survey coordinates were taken on each target location. Thermal "space" blankets (n = 20) and Coleman Sport catalytic heaters (n = 8) were used as the air targets. RTK was recorded for spatial reference at all corners of each thermal blanket and at every heater location. Final TIR mosaics were evaluated for spatial accuracy based on the location of these reference points on the imagery. The accuracy is expressed as root mean square error (RMSE) and was calculated by measuring the difference between air target RTK and the same location(s) on the TIR imagery. Figure 7 displays an air target location where both types of targets were set up, and demonstrates the accuracy of the imagery by comparing location of the target(s) with the RTK.

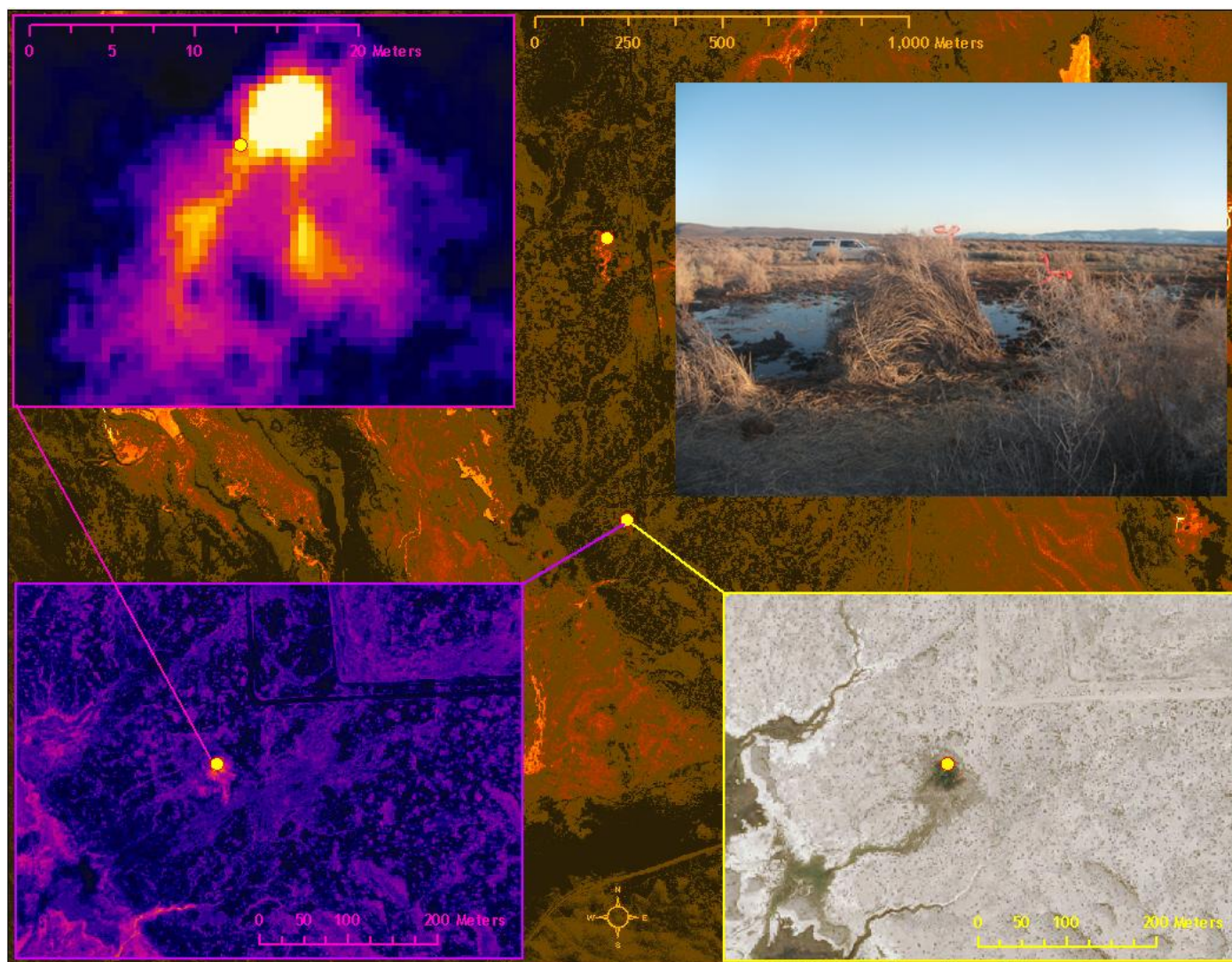
Figure 7. Air target location used for spatial accuracy assessment. The air target RTK locations are represented by the turquoise dots (blanket on the left and the single point over the heater is on the right) and a control monument is represented by the yellow triangle



2.4 Study Area Results

The objective of this project was to identify geothermal activity in the Summer Lake study area. Acquisition flights were conducted in pre-dawn hours to maximize the thermal contrast between the hot springs, seeps, and features with possible geothermal signatures from their surrounding cooler terrestrial environment. By flying early in the morning, residual thermal loading from the sun was minimized allowing the highest probability of detection for warmer features that would indicate near surface geo-thermal activity. Given the seasonality and time of acquisition, geothermal influenced land and water forms should be easily identifiable in the imagery.

Figure 8. Hobo Pro data logger location (SN 9951841) in the Summer Lake study area. The TIR images on the left side of the image show the thermal spatial variability around the logger location. The image in the upper right shows a ground level photo of the same location. The ground level photo illustrates that most pixels at this location will have mixed pixels and hence lower radiant temperatures



Thermal Infrared & LiDAR Remote Sensing: (DOGAMI) Summer Lake, OR

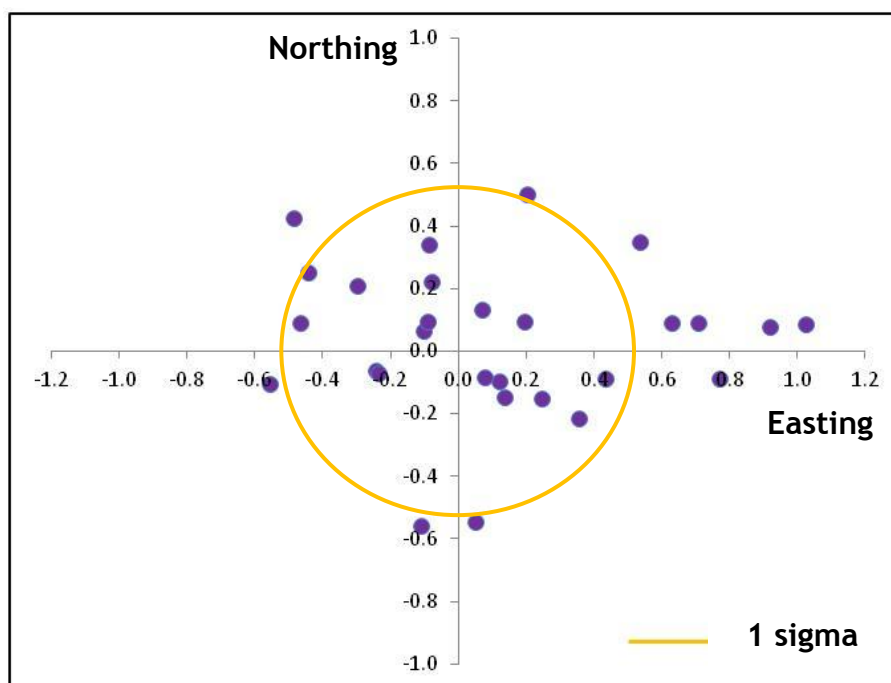
Prepared by Watershed Sciences, Inc.

2.4.1 Spatial Accuracy for Thermal Imagery

Table 4. Spatial Accuracy Assessment for Final TIR Mosaics of Summer Lake study area.

	Mean	Standard Deviation (1 Sigma)	Root Mean Square Error (RMSE)
Summer Lake TIR	0.12 m	0.49 m	0.50 m

Figure 9. Accuracy residuals from comparing RTK of air targets with locations on final thermal mosaics (units representing accuracy on both axes are in meters)



2.4.2 Thermal Accuracy Assessment

The radiant temperatures from the TIR images were compared to the kinetic temperatures measured using the data loggers at the time of the over flight (Table 5). For two locations (SN 2386978 and SN 9951845), radiant temperatures were ~1.2°C warmer than the kinetic temperatures. However, radiant temperatures were warmer for all other locations ranging in difference from 0.9°C to 4.0°C. Review of the imagery indicated that the two locations with warmer radiant temperatures were located in open water and presumably were our most reliable measurements. The other data loggers were located in smaller sources of water similar to the location illustrated in Figure 8. The cooler radiant temperatures at these locations and the variability in differences at the smaller sites were expected due to the probability of hybrid or mixed pixels. Consequently, interpretation of the TIR imagery should

consider that the actual temperatures of detected geothermal sources are probably greater than represented in the TIR imagery.

Table 5. Comparison of recorded temperatures measured at the time of the overflight compared to computed radiant temperatures

Sensor Serial #	UTC Time	Local Time	Kinetic °C	Radiant °C	Difference °C
2386978	13:29:10	5:29:10	10.7	12.0	-1.3
1026267	13:04:23	5:04:23	3.1	1.1	2.0
9951845	12:46:41	4:46:41	10.4	11.6	-1.2
9951841	11:09:41	3:09:41	13.7	9.7	4.0
9951842	10:45:44	2:45:44	12.4	11.5	0.9
9911293	10:26:42	2:26:42	5.5	2.0	3.5

The radiant temperatures for each ground truth location were checked in adjacent flight lines to check for any thermal drift in the sensor or acquisition conditions. This comparison resulted in differences of <0.2°C, which was well within the expected range for the sensor. We also visually assessed individual flight lines across the study area and observed very little change with individual flight lines not directly discernible in the thermal mosaic.

3. Light Detection and Ranging (LiDAR)

The LiDAR survey utilized a Leica ALS60 sensor in a Cessna Caravan. The Leica system was set to acquire 88,000 laser pulses per second (i.e., 88 kHz pulse rate) and was flown at 1,100 meters above ground level (AGL), capturing a scan angle of $\pm 15^\circ$ from nadir. With these flight parameters, the laser swath width is 598m and the laser pulse footprint is 26cm. These settings were developed to yield points with an average native pulse density of ≥ 4 pulses per square meter over terrestrial surfaces. It is not uncommon for some types of surfaces (e.g. dense vegetation or water) to return fewer pulses than the laser originally emitted. These discrepancies between 'native' and 'delivered' density will vary depending on terrain, land cover, and the prevalence of water bodies.

All areas were surveyed with an opposing flight line side-lap of $\geq 50\%$ ($\geq 100\%$ overlap) to reduce laser shadowing and increase surface laser painting. The Leica laser systems allow up to four range measurements (returns) per pulse, and all discernible laser returns were processed for the output dataset.

To accurately solve for laser point position (geographic coordinates x, y, z), the positional coordinates of the airborne sensor and the attitude of the aircraft were recorded continuously throughout the LiDAR data collection mission. Aircraft position was measured twice per second (2 Hz) by an onboard differential GPS unit. Aircraft attitude was measured 200 times per second (200 Hz) as pitch, roll and yaw (heading) from an onboard inertial measurement unit (IMU). To allow for post-processing correction and calibration, aircraft/sensor position and attitude data are indexed by GPS time.

3.1 Ground Survey - Instrumentation and Methods

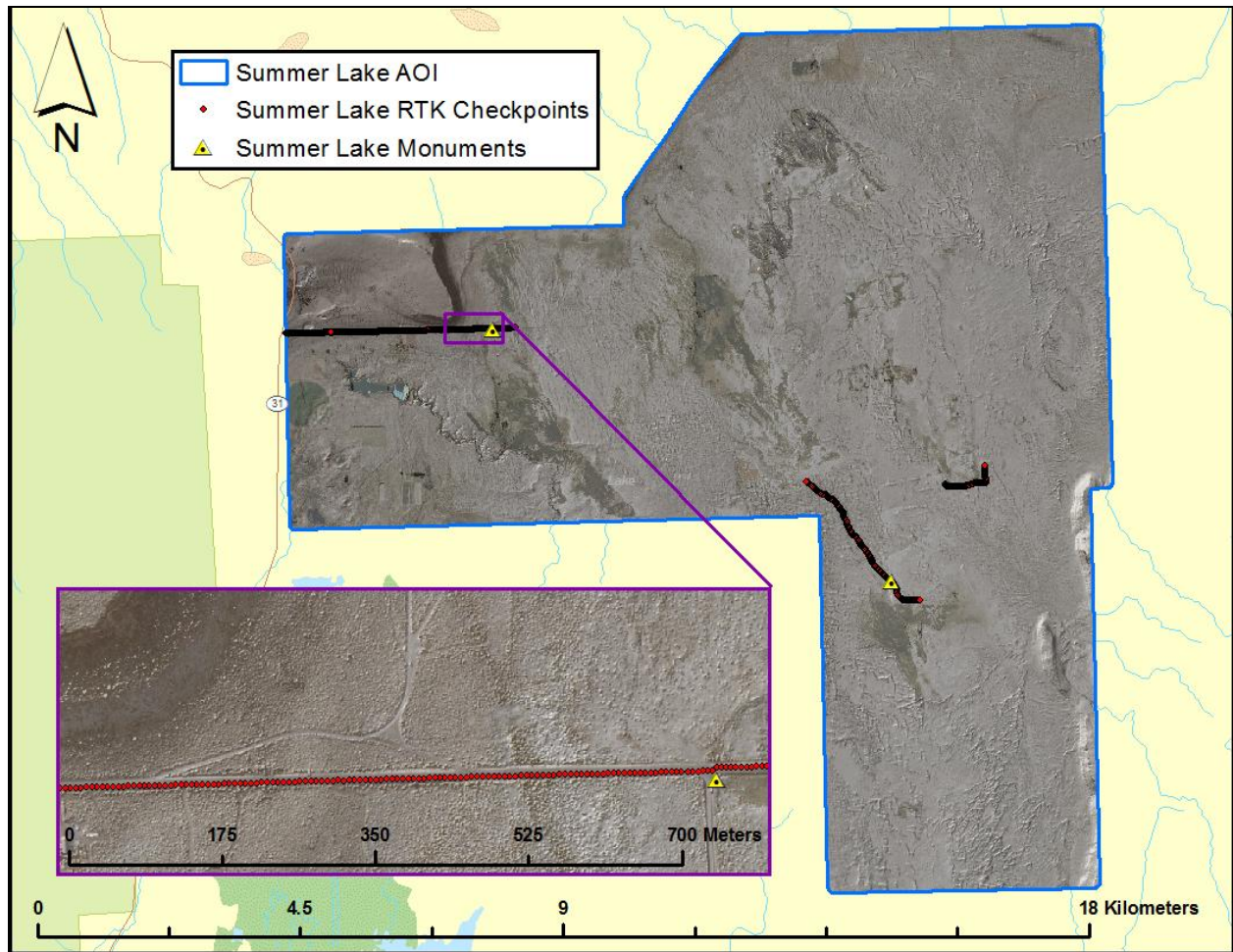
During the TIR and LiDAR surveys, static (1 Hz recording frequency) ground surveys were conducted over set monuments. Monument coordinates are provided in Table 2 and shown in Figure 10 for the Summer Lake study area. After the airborne survey, the static GPS data are processed using triangulation with Continuously Operating Reference Stations (CORS) and checked using the Online Positioning User Service (OPUS¹) to quantify daily variance. Multiple sessions were processed over the same monument to confirm antenna height measurements and reported position accuracy.

Indexed by time, these GPS data are used to correct the continuous onboard measurements of aircraft position recorded throughout the mission. Control monuments were located within 13 nautical miles of the surveyed area.



¹ Online Positioning User Service (OPUS) is run by the National Geodetic Survey to process corrected monument positions.

Figure 10. Survey control monument and RTK locations used in the Summer Lake study area



3.1.1 Methodology

The aircraft was assigned a ground crew member with two Trimble R7 receivers and an R8 receiver. All control monuments used for aerial acquisition were observed for a minimum of one survey session lasting no fewer than 4 hours and a second session lasting no fewer than 2 hours. At the beginning of every session the tripod and antenna were reset, resulting in two independent instrument heights and data files. Data was collected at a rate of 1Hz using a 10 degree mask on the antenna.

Aircraft mounted GPS measurements were made during periods with PDOP² less than or equal to 3.0 and with at least 6 satellites in view of a stationary reference receiver. Static GPS data collected in a continuous session average the high PDOP into the final solution in the method

²PDOP: Point Dilution of Precision is a measure of satellite geometry, the smaller the number the better the geometry between the point and the satellites.

used by CORS stations. RTK positions were collected on bare earth locations such as paved, gravel or stable dirt roads, and other locations where the ground is clearly visible (and is likely to remain visible) from the sky during the data acquisition and RTK measurement period(s). RTK measurements are not taken on highly reflective surfaces such as center line stripes or lane markings on roads. RTK points were taken no closer than one meter to any nearby terrain breaks such as road edges or drop offs.

The ground crew uploaded the GPS data to our FTP site for QA/QC review and processing in our office. OPUS processing triangulates the monument position using 3 CORS stations resulting in a fully adjusted position. After all data have been collected at each monument, accuracy and error ellipses are calculated from the OPUS reports. This information leads to a rating of the monument based on FGDC-STD-007.2-1998³ Part 2 table 2.1 at the 95% confidence level (St Dev_{NE}: 0.010 m, St Dev_Z: 0.010 m). When a statistically stable position is found CORPSCON⁴ 6.0.1 software is used to convert the UTM positions to geodetic positions. This geodetic position is used for processing the LiDAR data.

3.2 Data Processing

3.2.1 Applications and Work Flow Overview

1. Resolved kinematic corrections for aircraft position data using kinematic aircraft GPS and static ground GPS data.

Software: Waypoint GPS v.8.10, Trimble Business Center 2.6

2. Developed a smoothed best estimate of trajectory (SBET) file that blends post-processed aircraft position with attitude data. Sensor head position and attitude were calculated throughout the survey. The SBET data were used extensively for laser point and thermal image processing.

Software: IPAS TC v.3.1

3. Calculated laser point position by associating SBET position to each laser point return time, scan angle, intensity, etc. Created raw laser point cloud data for the entire survey in *.las (ASPRS v. 1.2) format. Data were then converted to orthometric elevations (NAVD88) by applying a Geoid03 correction.

Software: ALS Post Processing Software v.2.74

4. Imported raw laser points into manageable blocks (less than 500 MB) to perform manual relative accuracy calibration and filter for pits/birds. Ground points were then classified for individual flight lines (to be used for relative accuracy testing and calibration).

Software: TerraScan v.12.004

5. Using ground classified points per each flight line, the relative accuracy was tested. Automated line-to-line calibrations were then performed for system attitude parameters (pitch, roll, heading), mirror flex (scale) and GPS/IMU drift. Calibrations were performed on ground classified points from paired flight lines. Every flight line was used for relative accuracy calibration.

Software: TerraMatch v.12.001

³ Federal Geographic Data Committee Draft Geospatial Positioning Accuracy Standards

⁴ U.S. Army Corps of Engineers , Engineer Research and Development Center Topographic Engineering Center software

6. Position and attitude data were imported. Resulting data were classified as ground and non-ground points. Statistical absolute accuracy was assessed via direct comparisons of ground classified points.

Software: TerraScan v.12.004, TerraModeler v.12.002

7. Bare Earth models were created as a triangulated surface and exported as ArcInfo ASCII grids at a 1 meter pixel resolution. Highest Hit models were created for any class at 1 meter grid spacing and exported as ArcInfo ASCII grids.

Software: TerraScan v.12.004, TerraModeler v.12.002, ARCGIS10

3.2.2 Aircraft Kinematic GPS and IMU Data

LiDAR survey datasets were referenced to the 1 Hz static ground GPS data collected over pre-surveyed monuments with known coordinates. While surveying, the aircraft collected 2 Hz kinematic GPS data, and the onboard inertial measurement unit (IMU) collected 200 Hz aircraft attitude data. Waypoint GPS v.8.10 was used to process the kinematic corrections for the aircraft. The static and kinematic GPS data were then post-processed after the survey to obtain an accurate GPS solution and aircraft positions. IPAS TC v.3.1 was used to develop a trajectory file that includes corrected aircraft position and attitude information. The trajectory data for the entire flight survey session were incorporated into a final smoothed best estimated trajectory (SBET) file that contains accurate and continuous aircraft positions and attitudes.

3.2.3 Laser Point Processing

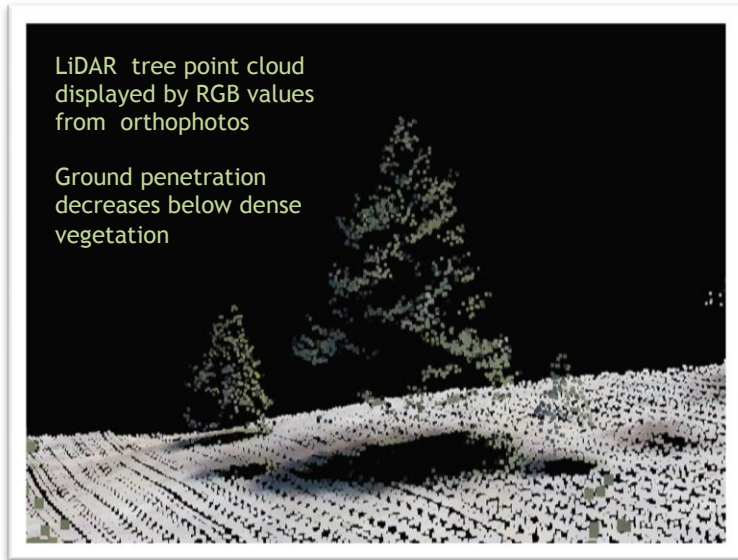
Laser point coordinates were computed using the IPAS and ALS Post Processor software suites based on independent data from the LiDAR system (pulse time, scan angle), and aircraft trajectory data (SBET). Laser point returns (first through fourth) were assigned an associated (x, y, z) coordinate along with unique intensity values (0-255). The data were output into large LAS v. 1.2 files with each point maintaining the corresponding scan angle, return number (echo), intensity, and x, y, z (easting, northing, and elevation) information.

These initial laser point files were too large for subsequent processing. To facilitate laser point processing, bins (polygons) were created to divide the dataset into manageable sizes (<500 MB). Flightlines and LiDAR data were then reviewed to ensure complete coverage of the survey area and positional accuracy of the laser points.

Laser point data were imported into processing bins in TerraScan, and manual calibration was performed to assess the system offsets for pitch, roll, heading and scale (mirror flex). Using a geometric relationship developed by Watershed Sciences, each of these offsets was resolved and corrected if necessary.

LiDAR points were then filtered for noise, pits (artificial low points), and birds (true birds as well as erroneously high points) by screening for absolute elevation limits, isolated points and height above ground. Each bin was then manually inspected for remaining pits and birds and spurious points were removed. In a bin containing approximately 7.5-9.0 million points, an average of 50-100 points are typically found to be artificially low or high. Common sources of non-terrestrial returns are clouds, birds, vapor, haze, decks, brush piles, etc.

Internal calibration was refined using TerraMatch. Points from overlapping lines were tested for internal consistency and final adjustments were made for system misalignments (i.e., pitch, roll, heading offsets and scale). Automated sensor attitude and scale corrections yielded 3-5 cm improvements in the relative accuracy. Once system misalignments were corrected, vertical GPS drift was then resolved and removed per flight line, yielding a slight improvement (<1 cm) in relative accuracy.



The TerraScan software suite is designed specifically for classifying near-ground points (Soininen, 2004). The processing sequence began by ‘removing’ all points that were not ‘near’ the earth based on geometric constraints used to evaluate multi-return points. The resulting bare earth (ground) model was visually inspected and additional ground point modeling was performed in site-specific areas to improve ground detail. This manual editing of ground often occurs in areas with known ground modeling deficiencies, such as: bedrock outcrops, cliffs, deeply incised stream banks, and dense vegetation. In some cases, automated ground point classification erroneously included known vegetation (i.e., understory, low/dense shrubs, etc.). These points were manually reclassified.

3.3 LiDAR Accuracy Assessment

3.3.1 Absolute Accuracy

Laser point absolute accuracy is largely a function of laser noise and relative accuracy. To minimize these contributions to absolute error, a number of noise filtering and calibration procedures were performed prior to evaluating absolute accuracy. The LiDAR quality assurance process uses the data from the real-time kinematic (RTK) ground survey conducted in the AOI. For the Summer Lake survey area, a total of **1038** RTK GPS measurements were collected. All measurements were collected on hard surfaces and distributed among multiple flight swaths. To assess absolute accuracy the location coordinates of these known RTK ground points were compared to those calculated for the closest ground-classified laser points.

The vertical accuracy of the LiDAR data is described as the mean and standard deviation (sigma ~ σ) of divergence of LiDAR point coordinates from RTK ground survey point coordinates. To provide a sense of the model predictive power of the dataset, the root mean square error (RMSE) for vertical accuracy is also provided. These statistics assume the error distributions for x, y, and z are normally distributed, thus the skew and kurtosis of distributions are considered when evaluating error statistics.

Statements of statistical accuracy apply to fixed terrestrial surfaces only and may not be applied to areas of dense vegetation or steep terrain (See Appendix A).

3.3.2 LiDAR Data Summary

Summary statistics for point resolution and accuracy (relative and absolute) of the LiDAR data collected in the Summer Lake study area are presented below in terms of central tendency, variation around the mean, and the spatial distribution of the data. The initial LiDAR dataset, acquired to be ≥ 4 points per square meter was filtered as described previously to remove spurious or inaccurate points. Additionally, some types of surfaces (i.e., dense vegetation, breaks in terrain, water, steep slopes, and highly reflective rock surfaces) may return fewer pulses (delivered density) than the laser originally emitted (native density).

Ground classifications were derived from automated ground surface modeling and manual, supervised classifications where it was determined that the automated model had failed. Ground return densities will be lower in areas of dense vegetation, water, or buildings.

Table 6. Resolution and Accuracy - Specifications and Achieved Values

	Targeted	Achieved
Resolution:	≥ 4 points/m ²	5.43 points/m ²
Vertical Accuracy (1 σ):	<15 cm	2.32 cm

LiDAR data resolution:

- Average Point (First Return) Density = **5.43 points/m²**
- Average Ground Point Density = **2.35 points/m²**

3.3.3 LiDAR Relative Accuracy Calibration Results

Relative accuracy statistics for the Summer Lake study area measure the full survey calibration including areas outside the delivered boundary:

- Project Average = 0.04m
- Median Relative Accuracy = 0.04m
- 1 σ Relative Accuracy = 0.01m
- 1.96 σ Relative Accuracy = 0.01m
- RMSE = 0.01m

3.3.4 LiDAR Absolute Accuracy

Table 7. Absolute Accuracy - Deviation between laser points and RTK hard surface survey points

RTK Survey Sample Size (n):1,038		
Root Mean Square Error (RMSE):0.02m		Minimum Δz :-0.07m
Standard Deviations		Maximum Δz : 0.08m
1 sigma (σ): 0.02m	1.96 sigma (2σ): 0.04m	Average Δz : 0.00m

4. Projection/Datum and Units

Projection:		UTM Zone 10N
Datum	Vertical:	NAVD88 Geoid 03
	Horizontal:	NAD 83 (Cors96)
Units:		Meters

5. Deliverables

5.1 TIR Deliverables

Raster Data:	<ul style="list-style-type: none">• <i>TIR mosaic</i> (GEOTiff format)<ul style="list-style-type: none">▪ total survey boundary mosaic▪ 7.5" quad delineation mosaics• <i>Rectified Thermal Frames</i> (GEOTiff format)<ul style="list-style-type: none">▪ Full Delivery Boundary mosaic▪ 0.75" quad delineation• <i>Unrectified Thermal Frames</i> (Imagine .img format 640 x 512 pixels)
Vector Data:	<ul style="list-style-type: none">• <i>Image Frame Index</i> The actual image frame (or event) locations. The file shows the flight line locations and image times.
Data Report:	<ul style="list-style-type: none">• Full report containing introduction, methodology, and accuracy

5.2 LiDAR Deliverables

Point Data:	<ul style="list-style-type: none">• <i>Ground Classified</i> (0.75" quad delineation LAS 1.2 format)• <i>All Returns</i> (0.75" quad delineation LAS 1.2 format)
Vector Data	<ul style="list-style-type: none">• <i>0.75" Quad Tile Index</i> for LiDAR Points (ESRI shapefile format and DGN)• <i>7.5" Quad DEM Index</i> (ESRI shapefile format)• <i>Survey Boundary</i> (Total Area Flown) (ESRI shapefile format)
Raster Data:	<ul style="list-style-type: none">• <i>Bare Earth DEM</i> (7.5" quad delineation ESRI grid format)• <i>Highest Hit DEM</i> (7.5" quad delineation ESRI grid format)• <i>Intensity Images</i> (0.75" quad delineation GEOTiff format)

6. Certifications

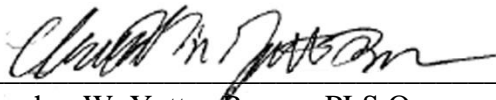
Watershed Sciences provided LiDAR services for the DOGAMI: Summer Lake study area as described in this report.

I, Russ Faux, have reviewed the attached report for completeness and hereby state that it is a complete and accurate report of this project.

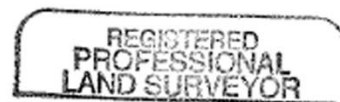


Russ Faux
Principal
Watershed Sciences, Inc.

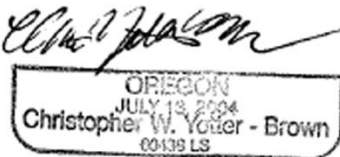
I, Christopher W. Yotter-Brown, being first dully sworn, say that as described in the Ground Survey subsection of the Acquisition section of this report was completed by me or under my direct supervision and was completed using commonly accepted standard practices. Accuracy statistics shown in the Accuracy Section have been reviewed by me to meet National Standard for Spatial Data Accuracy.



Christopher W. Yotter-Brown, PLS Oregon & Washington
Watershed Sciences, Inc
Portland, OR 97204



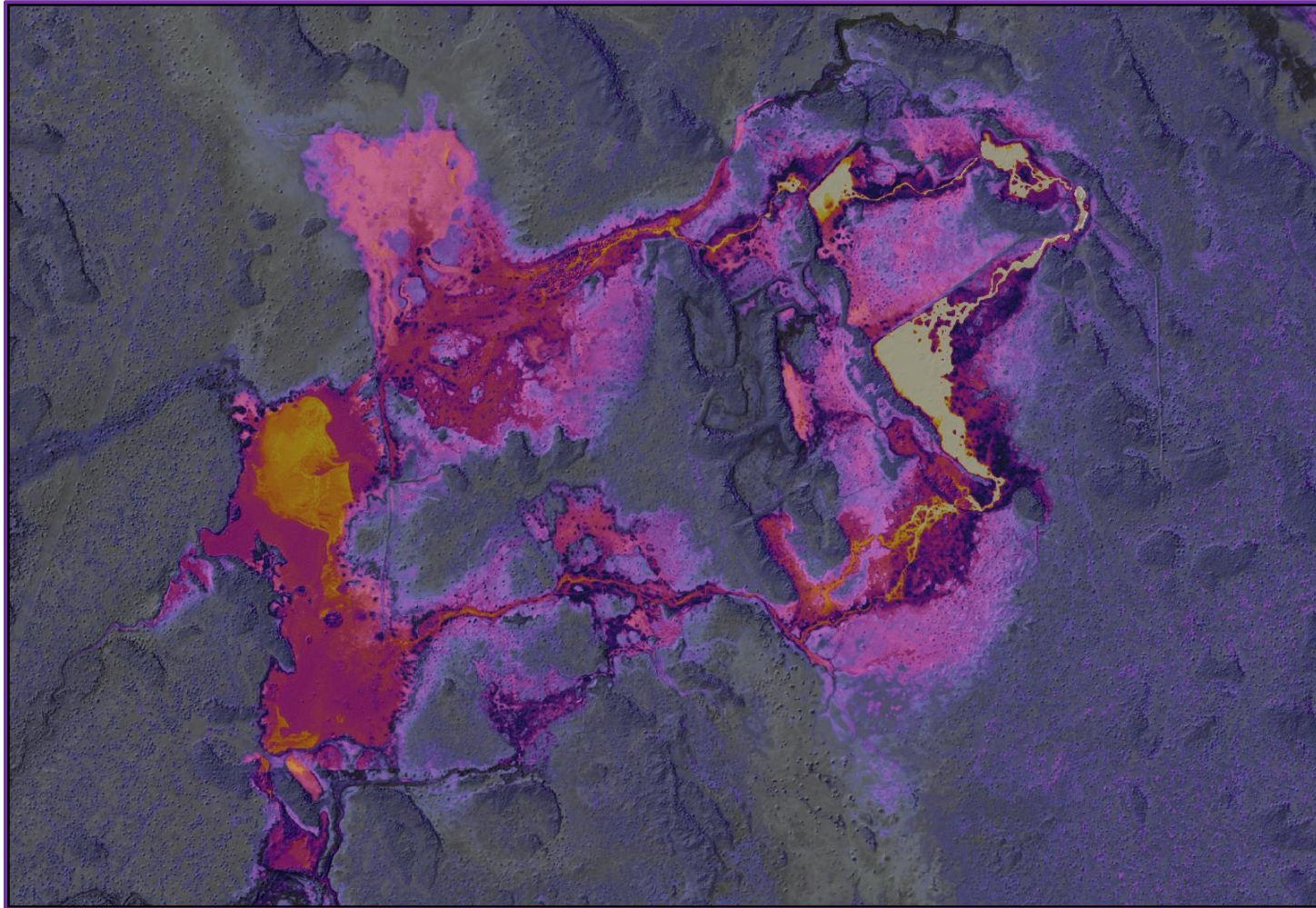
5/14/2012



RENEWAL DATE: 6/31/2012

7. Selected Images

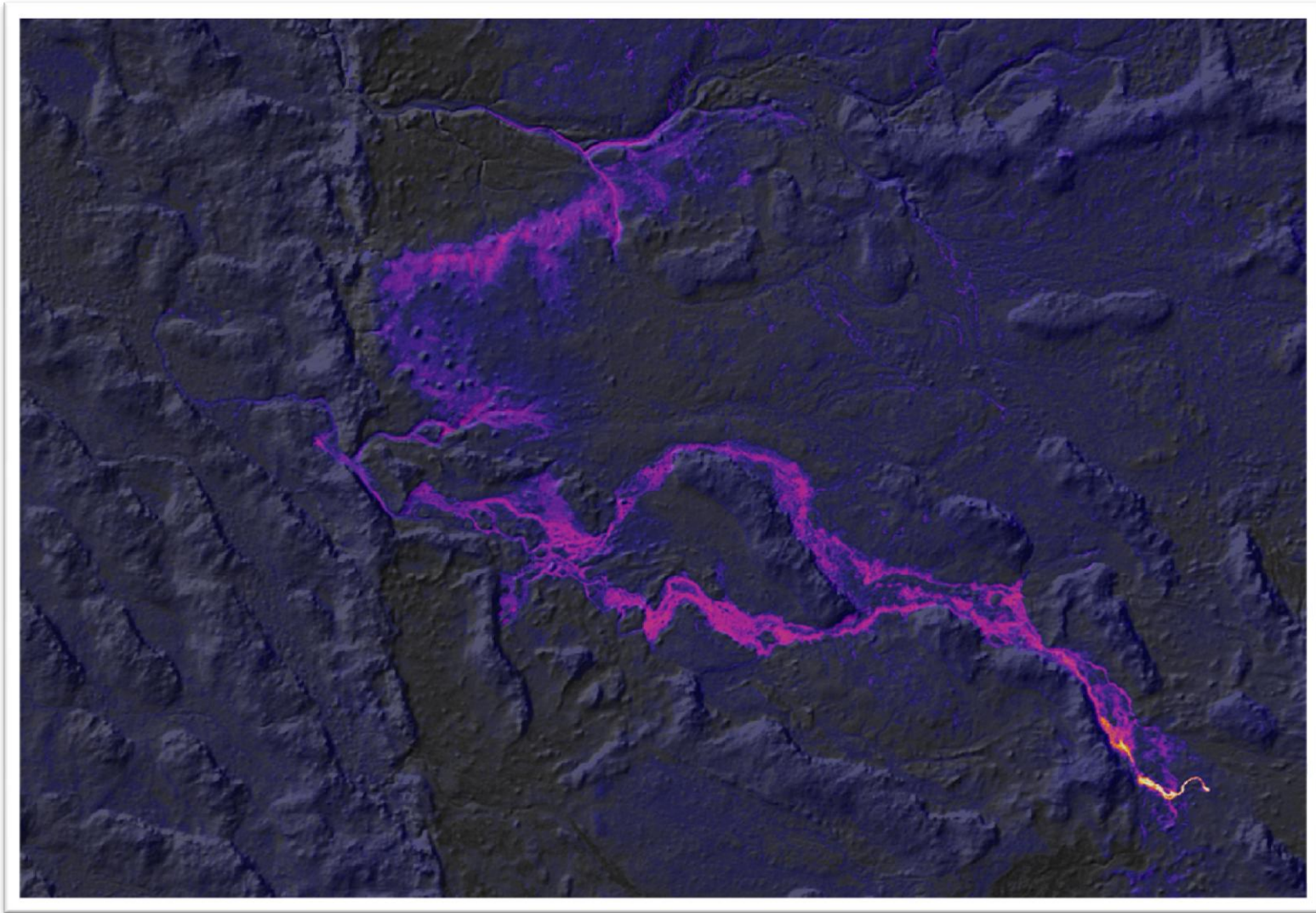
Figure 11. Aerial view of an isolated desert spring off of Thousand Springs Lane in Lake County, Oregon. Image is a thermal mosaic GEOTiff with a project specific color ramp draped over 2011 NAIP imagery and the LiDAR generated Highest Hit DEM.



Thermal Infrared & LiDAR Remote Sensing: (DOGAMI) Summer Lake, OR

Prepared by Watershed Sciences, Inc.

Figure 12. Isolated desert spring in the Summer Lake study area off of Thousand Springs Ln. (Co. Hwy 4-17). Image is a thermal mosaic GEOTiff with a project specific color ramp to enhance the temperature variation found in the data.



Thermal Infrared & LiDAR Remote Sensing: (DOGAMI) Summer Lake, OR

Prepared by Watershed Sciences, Inc.

Figure 13. Aerial view looking southwest toward the town of Summer Lake, Oregon across Carlon Lane. Image is a thermal mosaic draped over the LiDAR generated Highest Hit hillshade DEM. Note that the butte on the right side of the image has a warmer apparent temperature than the valley. The LIDAR model provides a very good tool for interpretation of these patterns with respect to geology and aspect. We believe that the rocks on the butte have retained some residual heat from the day.

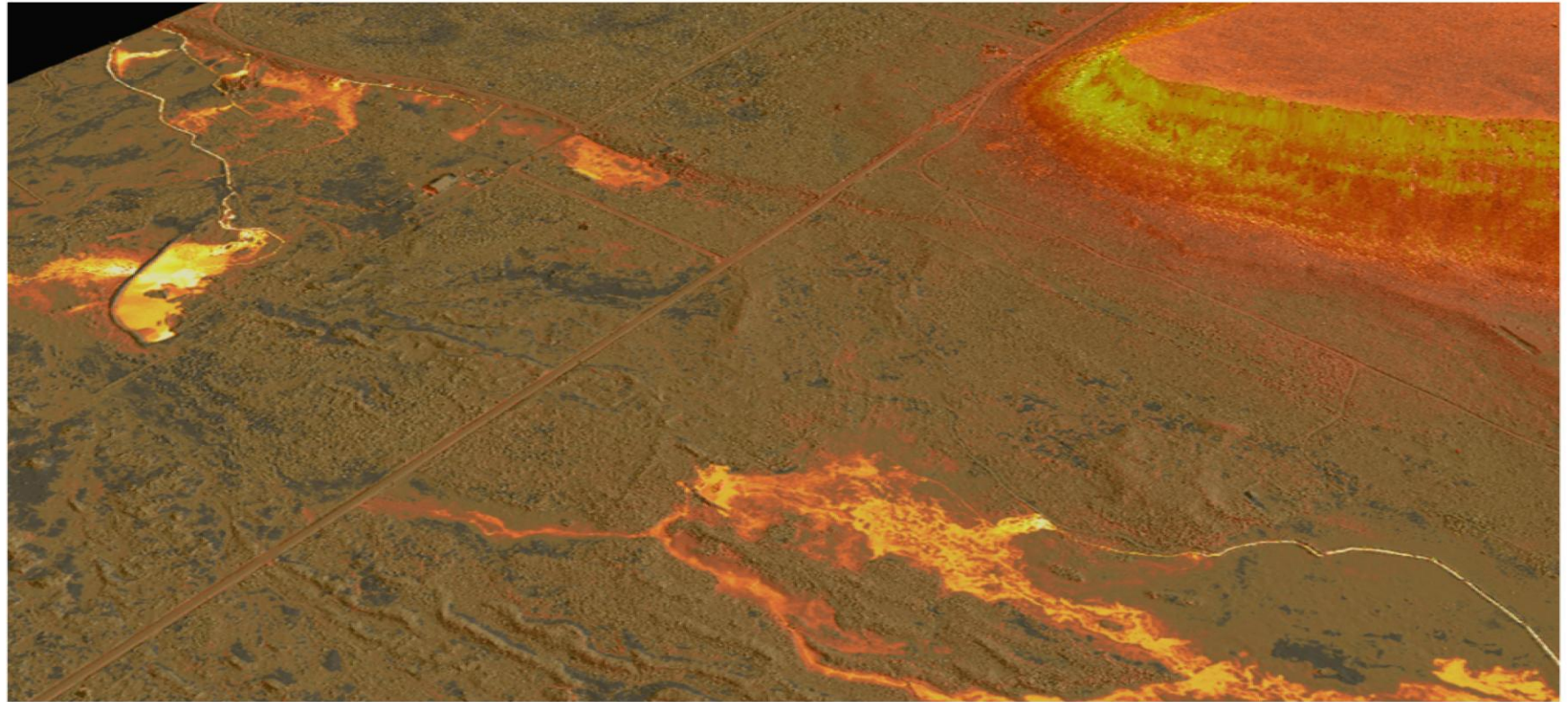


Figure 14. Aerial view looking to the southeast over Thousand Springs Lane (Co. Hwy 4-17) at several springs, and lacustrine deposit formations found in the Summer lake study area. Image is a thermal mosaic draped over the LiDAR generated Highest Hit hillshade DEM.

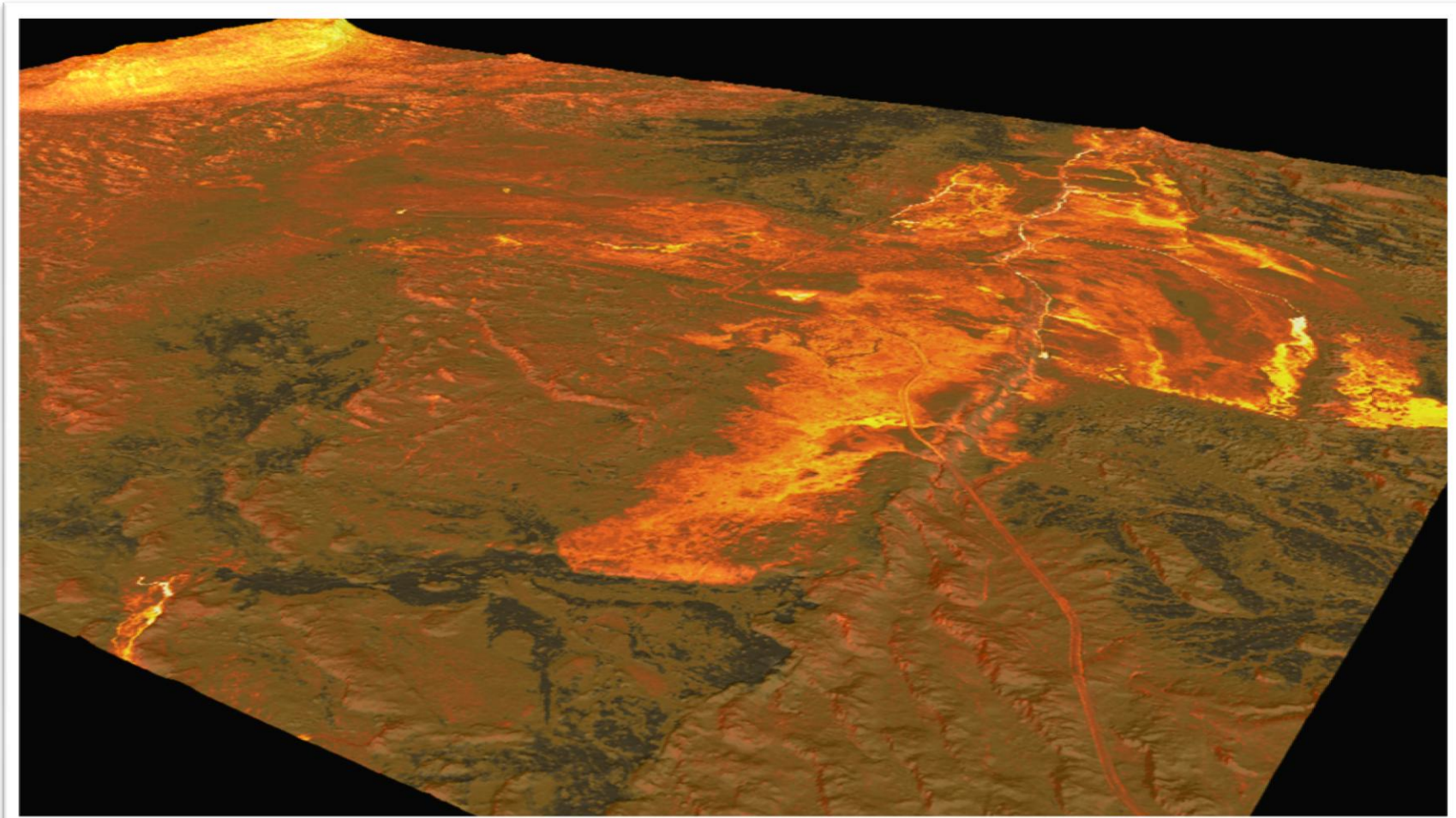
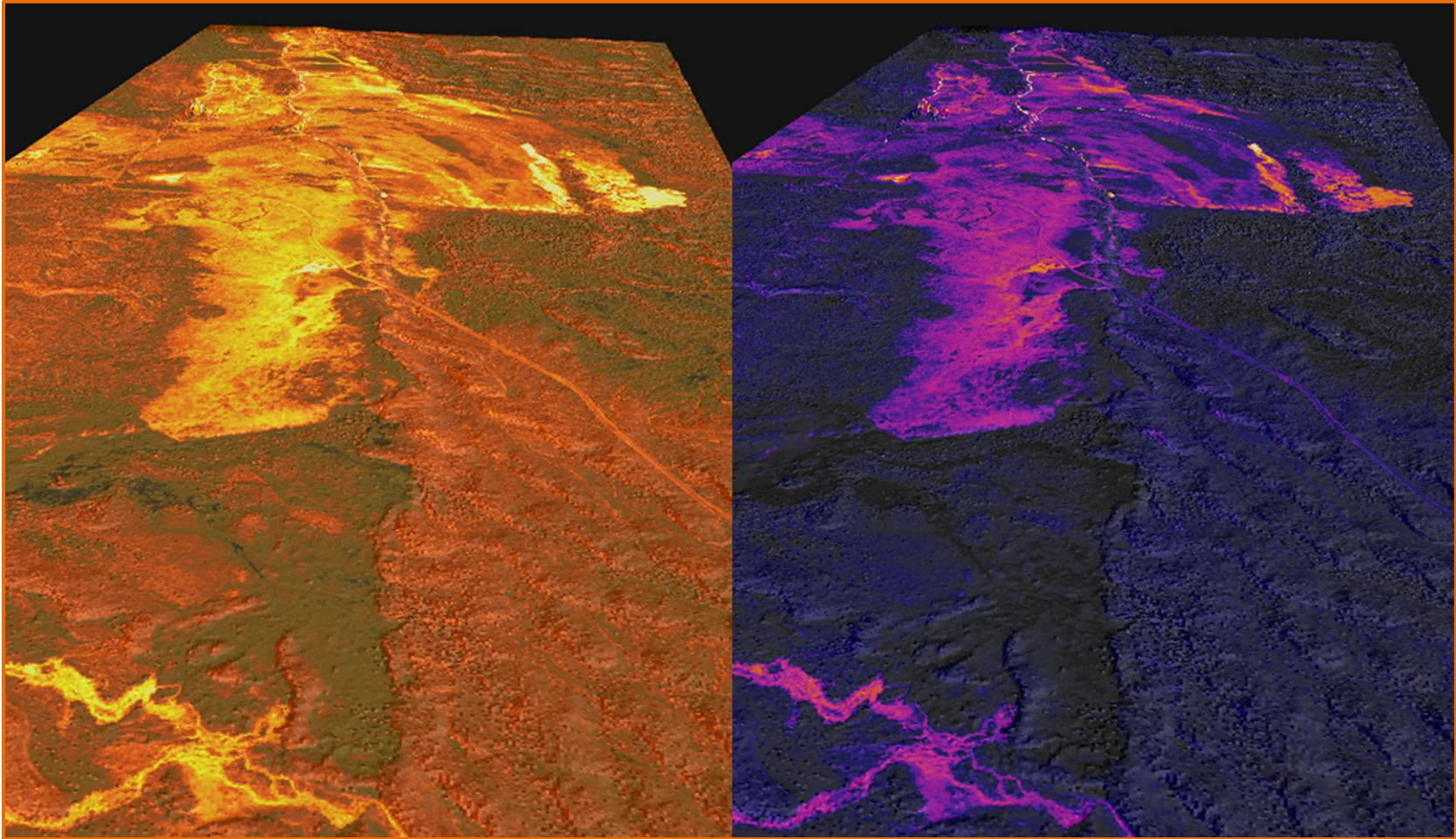


Figure 15. Aerial view looking south-southeast at the same spring complex in Figure 14, but from a different vantage point. The image was selected to enhance the view of the fault running through the region versus the old lake bed deposits and landforms. Images are thermal mosaics draped over the LiDAR generated Highest Hit hillshade DEM.



8. Glossary

1-sigma (σ) Absolute Deviation: Value for which the data are within one standard deviation (approximately 68th percentile) of a normally distributed data set.

1.96-sigma (σ) Absolute Deviation: Value for which the data are within two standard deviations (approximately 95th percentile) of a normally distributed data set.

Root Mean Square Error (RMSE): A statistic used to approximate the difference between real-world points and the LiDAR points. It is calculated by squaring all the values, then taking the average of the squares and taking the square root of the average.

Pulse Rate (PR): The rate at which laser pulses are emitted from the sensor; typically measured as thousands of pulses per second (kHz).

Pulse Returns: For every laser pulse emitted, the Leica ALS 50 Phase II system can record *up to four* wave forms reflected back to the sensor. Portions of the wave form that return earliest are the highest element in multi-tiered surfaces such as vegetation. Portions of the wave form that return last are the lowest element in multi-tiered surfaces.

Accuracy: The statistical comparison between known (surveyed) points and laser points. Typically measured as the standard deviation (sigma, σ) and root mean square error (RMSE).

Intensity Values: The peak power ratio of the laser return to the emitted laser. It is a function of surface reflectivity.

Data Density: A common measure of LiDAR resolution, measured as points per square meter.

Spot Spacing: Also a measure of LiDAR resolution, measured as the average distance between laser points.

Nadir: A single point or locus of points on the surface of the earth directly below a sensor as it progresses along its flight line.

Scan Angle: The angle from nadir to the edge of the scan, measured in degrees. Laser point accuracy typically decreases as scan angles increase.

Overlap: The area shared between flight lines, typically measured in percents; 100% overlap is essential to ensure complete coverage and reduce laser shadows.

DTM / DEM: These often-interchanged terms refer to models made from laser points. The digital elevation model (DEM) refers to all surfaces, including bare ground and vegetation, while the digital terrain model (DTM) refers only to those points classified as ground.

Real-Time Kinematic (RTK) Survey: GPS surveying is conducted with a GPS base station deployed over a known monument with a radio connection to a GPS rover. Both the base station and rover receive differential GPS data and the baseline correction is solved between the two. This type of ground survey is accurate to 1.5 cm or less.

9. Citations

Soininen, A. 2004. TerraScan User's Guide. TerraSolid.